



# Simultaneous determination of enthalpy of mixing and reaction using milli-scale continuous flow calorimetry

Finn L. Steinemann<sup>1</sup> · David P. Rützi<sup>1</sup> · Marlies Moser<sup>2</sup> · Alain G. Georg<sup>2</sup> · Daniel M. Meier<sup>1</sup>

Received: 24 May 2022 / Accepted: 12 July 2022  
© The Author(s) 2022

## Abstract

A simultaneous determination of the enthalpy of mixing and reaction in a scalable continuous milli-scale flow calorimeter is investigated. As obtained calorimetric data is pivotal for the safety assessment of chemical reactions and processes. The acid-catalysed selective, homogeneous hydrolysis of acetic anhydride with half-lives from a few seconds to a few minutes is investigated as a model reaction. For the enthalpy of mixing  $7.2 \pm 2.8$  kJ/mol and for the enthalpy of reaction  $-60.8 \pm 2.5$  kJ/mol were determined. For reactions that show complete conversion in the continuous reactor, a technique is introduced to further improve the accuracy of the reaction enthalpy determination. Thereby, the resolution of the observed temperature profile is increased by measuring the profile at different flow rates. Applying this procedure, the reaction enthalpy of  $-62.5$  kJ/mol was determined which is in good agreement with literature values for this model reaction.

**Keywords** Continuous flow calorimetry · Polytropic reaction calorimetry · Heat of reaction · Hydrolysis of acetic anhydride · Process development · Scale-up

## Introduction

Today, mainly batch reactors are used to produce fine chemicals in the range of up to 100 t/y [1]. As the industry is striving for process intensification, the changeover from a multifunctional batch plant to a smaller continuous monoplant can make economic sense, as there is no need for cleaning, charge and discharge [2]. In addition, continuous reactors are smaller for the same production capacity since higher temperatures and pressures allow a shorter residence time than batch reactors [3]. The heat transfer is better in a continuous flow reactor and there is less potential chemical energy, so the consequences of an incident are drastically reduced [4]. For the

safety assessment of a process, the determination of the enthalpy of reaction is an elementary component [5, 6]. The closer this determination is to the industrial process, the more robust safety data are obtained. For example, Mortzfeld et al. [7] found deviations in non-selective reactions when they were investigated using batch calorimeters or continuous flow calorimeters. Several flow calorimeters have been developed measuring the enthalpy of reaction using thermoelectric heat flow [8–10], infrared thermography [11], or segmental temperature sensors [7].

Recently, we have shown that the reaction enthalpy of a fast and selective reaction can be measured in the continuous flow calorimeter without extensive calibration of the heat transfer coefficient [12]. However, organometallic reactions, nitrations or polymerisations have half-lives in the range of seconds or minutes [13]. If full conversion is not achieved, the analysis of the exiting product is indispensable. Therefore, infrared spectroscopy is a suitable method of analysis due to its sensitivity, economic viability, and broad application possibilities [14, 15]. Furthermore, the enthalpy of mixing must be quantified since the conversion of the reaction is not complete and influences the calorimetric data. To determine the enthalpy of mixing, the heat of reaction in relation to the conversion must be known. In a batch calorimeter, the conversion can be determined over time and known kinetics [16] or inline measurements [17]. Ładosz et al. [18] have shown

## Highlights

- Simultaneous determination of enthalpy of mixing and heat of reaction using a flow calorimeter.
- Facile and fast flow screening procedure for accurate calorimetric data.
- Safe and scalable setup combined with online reaction monitoring.

✉ Daniel M. Meier  
meid@zhaw.ch

<sup>1</sup> School of Engineering, Institute of Materials and Process Engineering, ZHAW Zurich University of Applied Sciences, Technikumstrasse 9, 8401 Winterthur, Switzerland

<sup>2</sup> Fluitec mixing + reaction solutions AG, Seuzachstrasse 40, 8413 Neftenbach, Switzerland

that this determination of the enthalpy of mixing is possible in a continuous micro reactor at steady state under isothermal conditions.

In this work we aim to simultaneously investigate the heat of reaction and the enthalpy of mixing for the hydrolysis of acetic anhydride in a scalable continuous flow calorimeter. This model reaction has served for several continuous [18] and batch [16, 17, 19–21] calorimetric studies and is particularly suitable because the reaction rate can simply be tuned by the help of the acid concentration, which catalyses the reaction. A milli-scale continuous flow calorimeter, scalable to production scale, as used by us [12] is applied. Compared to other reactor setups to determine the enthalpy of reaction, for example Ładosz et al. [18], who used three temperature sensors, this calorimeter measures the temperature profile using ten temperature sensors. Even though the temperature profile is not indicated gapless, we report that a continuous indication is not necessary since the resolution of the temperature profile can be increased with different flow rates and the obtained data are highly reliable.

## Materials and methods

### Experimental setup

The experimental setup is shown in Fig. 1 and described in a recent publication [12], a picture of the experimental setup is

provided in the [supplementary information](#). Briefly, two piston pumps, dosing system 1 and 2 (DZRP-200, 63,639, Fluitec mixing + reaction solutions AG, Switzerland), were used to convey the feed streams. Both liquid feeds were conditioned to 20 °C in separate lines using a thermostat, Thermostat 1 (Ministat 230, Peter Huber Kältemaschinenbau AG, Germany). Before entering the flow calorimeter, the temperature was measured inline with a temperature probe immersed into the feed (Class A, Pt-100, 53,286, Fluitec). The reaction started immediately after mixing the two feeds in the flow calorimeter ( $L = 500$  mm,  $D_i = 12.3$  mm,  $V = 44.3$  ml Contiplant PFR-50-SS, Fluitec), which was equipped with a pre-mixer, static CSE-X mixers and 10 axial temperature sensors (Class 1, type K, Fluitec). Prior the experiments, the axial temperature sensors were calibrated at 20, 30, 40, 50, 60, 70 and 80 °C. In addition, the equilibrated temperatures recorded by the sensors were compared to the heat transfer medium (HTM) temperature, measured with a class A temperature sensor before each experiment. No temperature drift was detected during the measurement period.

At the outlet of the flow calorimeter, the reaction solution was analysed in-line with a Fourier transform infrared spectrometer (FTIR) equipped with a liquid cell and a hold up volume of 0.3 ml (Alpha II, Bruker Corporation, USA). After passing through the backpressure regulator (Contiplant valve, 64,144, Fluitec), the liquid was collected and neutralised. Water was used as HTM, which was tempered and circulated by a thermostat, Thermostat 2 (CC304, Peter Huber). A Coriolis mass flow meter (Promass 80F15, Endress

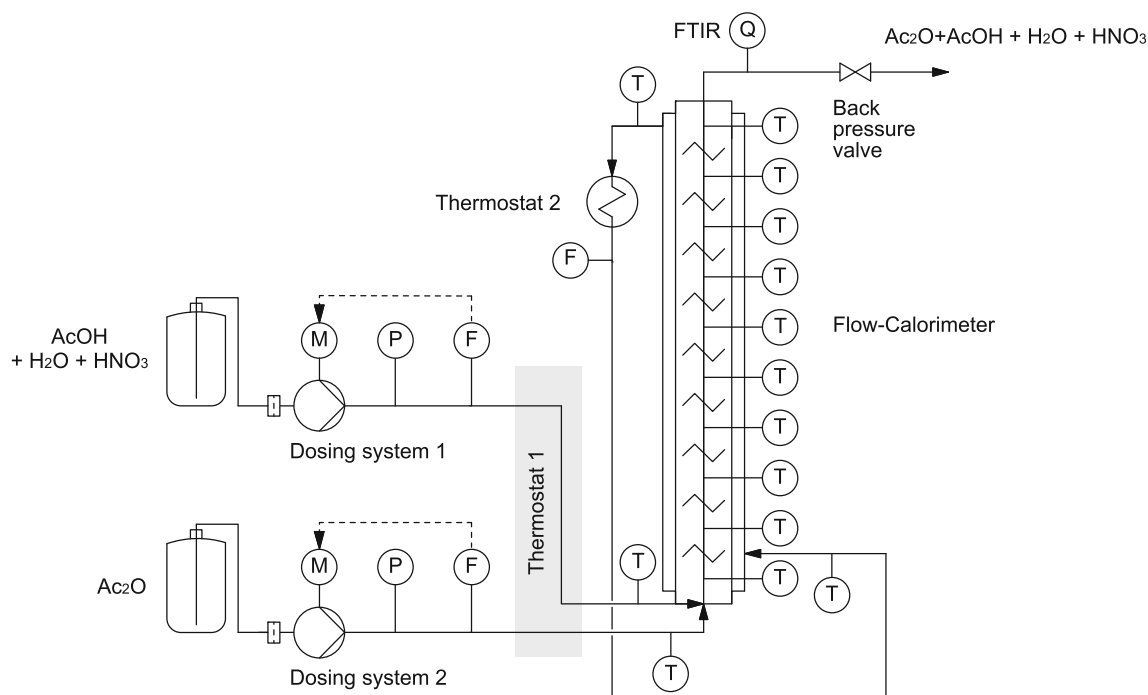


**Fig. 1** Schematic of the setup of the continuous flow calorimeter. The feeds contain acetic anhydride (Ac<sub>2</sub>O) and acetic acid (AcOH), Water (H<sub>2</sub>O) and nitric acid (HNO<sub>3</sub>), respectively

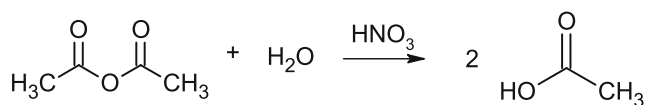


**Fig. 2** Reaction equation of the hydrolysis of acetic acid anhydride,  $\text{HNO}_3$  is used as catalyst

+ Hauser (Schweiz) AG, Switzerland) recorded the mass flow of the HTM.

Temperatures, flow rates and pressures were recorded every second using a Siemens S7 control system. The reaction solution at the outlet was analysed by FTIR every 6.2 seconds.

## Hydrolysis of acetic anhydride

The selective acid catalysed hydrolysis of acetic anhydride ( $\text{Ac}_2\text{O}$ ) to acetic acid ( $\text{AcOH}$ ), shown in Fig. 2, served as the model reaction for this study. Importantly, the reaction rate can be easily adjusted by varying the catalyst concentration. As the reaction has been studied as a model reaction by several research groups, [16–22], the results can be well compared.

In order to estimate the operating range of continuous flow calorimetry, we introduced a flow factor  $\beta$  in a recent publication for the present reactor [12]. The product of the adiabatic temperature increase  $\Delta T_{\text{ad}}$  and the volume flow  $\dot{V}$  should be at least 200 K ml/min for an accurate determination of heat of reaction. The flow factor  $\beta$  was estimated to a range between 1700 and 8400 K ml/min for this reaction, fulfilling well the requirement.

## Experimental procedure

The flow calorimetry experiments were performed using  $\text{Ac}_2\text{O}$  and an aqueous solution (AS) containing  $\text{AcOH}$  and nitric acid ( $\text{HNO}_3$ ) at different concentrations (Table 1). In the AS solution, acetic acid ( $\text{AcOH}$ , Honeywell International Inc., puriss) was added because acetic anhydride ( $\text{Ac}_2\text{O}$ , Honeywell International Inc., puriss) no longer dissolved in water at the concentrations used. The reaction rate was adjusted by the concentration of  $\text{HNO}_3$  (65%, Roth AG, purum). Two experimental series were conducted with a lower catalyst concentration (E1 and E2) and two with a higher catalyst concentration (E3 and E4).

**Table 1** List of the components and their concentration in the feeds. Acetic anhydride was used undiluted, which corresponds to a concentration of 10.52 mol/l

	Compound	E1	E2	E3	E4
aqueous solution (AS)	$\text{HNO}_3$ [mol/l]	2.17	2.57	5.32	5.32
	$\text{H}_2\text{O}$ [mol/l]	35.5	33.6	28.5	28.6
	$\text{AcOH}$ [mol/l]	5.46	5.73	5.56	5.54
acetic anhydride ( $\text{Ac}_2\text{O}$ )	$\text{Ac}_2\text{O}$ [mol/l]	10.52	10.52	10.52	10.52

For the determination of conversion, five  $\text{Ac}_2\text{O}$  standard solutions with concentrations between 0.3 and 5 mol/l in  $\text{AcOH}$  were measured by FTIR and served as calibration. The conversion was then determined by analysing the baseline corrected FTIR signal of the reaction solution where the signal at 1125  $1/\text{cm}$  was identified as a fingerprint signal for  $\text{Ac}_2\text{O}$  (supplementary information).

To ensure a constant temperature in the calorimeter, the thermostats were started at least 30 min before the pumps. The total flow rates of the experiments are listed in Table 2, where the flow rate ratio between  $\text{Ac}_2\text{O}$  and AS is 8:10. The HTM was circulated at approximately 517 kg/h and set to 20 °C, the backpressure valve was set to 1 bar.

## Determination of the heat of reaction

The heat of reaction was determined as explained in [12] and is therefore only summarised here. The temperature profile is linearly interpolated and divided into 1000 segments, allowing a precise calculation of the exchanged power. The sum of the exchanged power  $\dot{Q}_{\text{ex}}$  and non-exchanged power  $\dot{Q}_{\text{nex}}$  is equal to the chemically generated power  $\dot{Q}_r$ .

$$0 = \frac{dQ}{dt} = \dot{Q}_r - \dot{Q}_{\text{ex}} - \dot{Q}_{\text{nex}} \quad (1)$$

If the product of the mass flow  $\dot{m}$ , the heat capacity  $c_p$ , and the temperature difference  $\Delta T_j$  between the initial and final temperature of the segment is summed over each segment, the non-exchanged power can be calculated

$$\dot{Q}_{\text{nex}} = \sum_{j=1}^n \dot{m} \cdot c_p \cdot \Delta T_j \quad (2)$$

Using the same summation, the exchanged power can be calculated from the heat transfer coefficient  $k$ , the segment shell area  $A$  and the temperature difference  $\Delta T_j$  between HTM and reaction solution.

$$\dot{Q}_{\text{ex}} = \sum_{j=1}^n k \cdot A \cdot \Delta T_j \quad (3)$$

**Table 2** Total volumetric flow  $\dot{V}$  of the conducted experiments. E2, 18 ml/min was performed in duplicates

$\dot{V}$ E1 [ml/min]	$\dot{V}$ E2 [ml/min]	$\dot{V}$ E3 [ml/min]	$\dot{V}$ E4 [ml/min]
18	18	18	44
36	36	36	48
54	54	54	52
72	72	72	56
90			60
			64
			68
			72

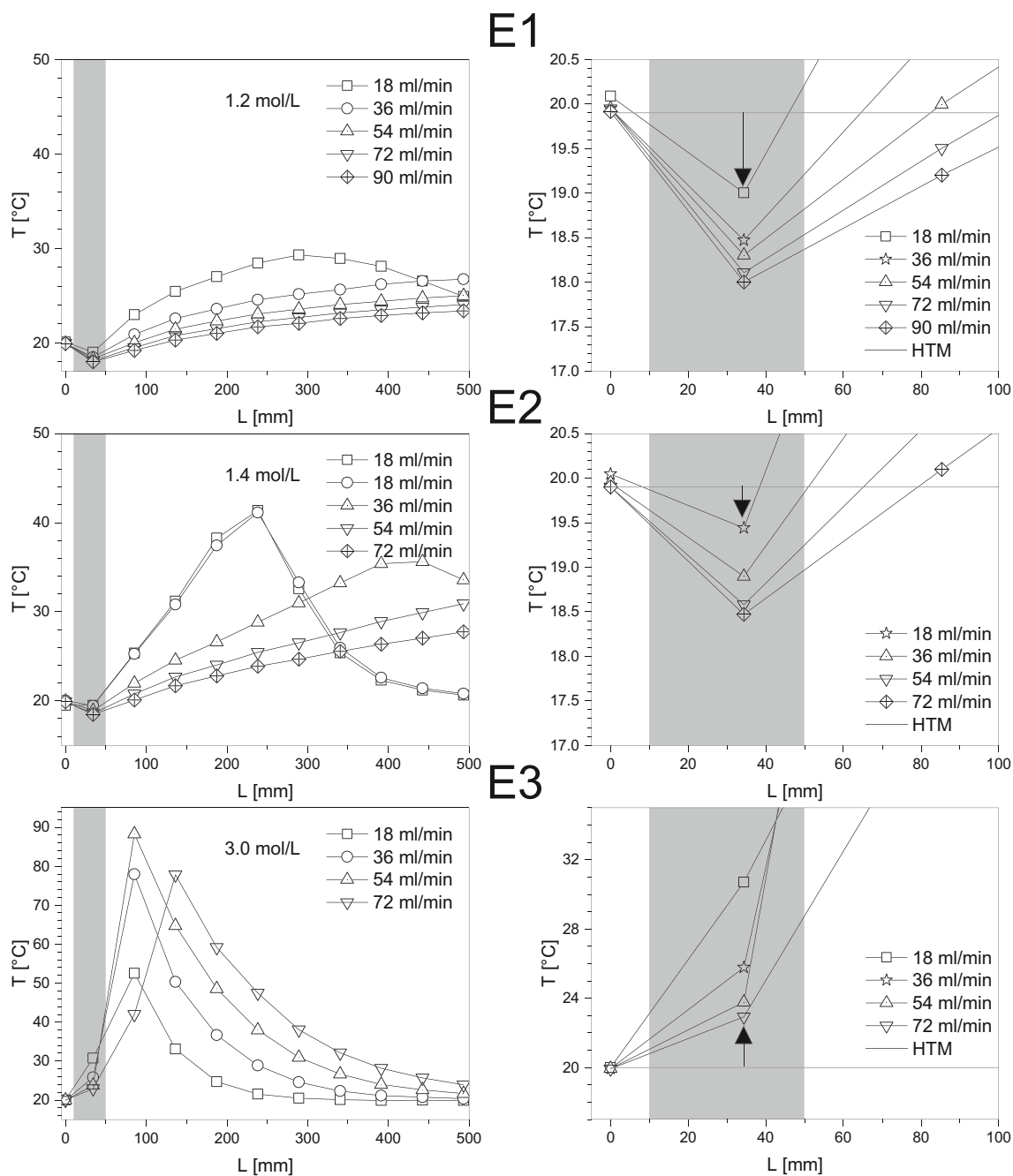


**Fig. 3** Left: Temperature profiles obtained from experimental series E1–E3. The maximum temperature reached is strongly dependent on the amount of catalyst and thus on the reaction rate. Right: Highlighted are

the temperature drops compared to the HTM-temperature at the beginning of the slower reactions due to the enthalpy of mixing

Since  $\dot{Q}_{\text{nex}}$  and  $\dot{Q}_{\text{ex}}$  are known from eqs. 2 and 3, the reaction power can now be determined using eq. 1. With the mass flow  $\dot{m}$  and the reaction power, the specific heat of reaction  $Q_r$  can now be calculated.

$$Q_r = \frac{\dot{Q}_{\text{ex}} + \dot{Q}_{\text{nex}}}{\dot{m}} \quad (4)$$

The exo- or endothermicity of a reaction is given by the enthalpy of reaction  $\Delta H_r$ . This can be calculated with eq. 5 from the heat of reaction  $Q_r$ , the density  $\rho$  and the molar concentration of the limiting acetic anhydride  $c_{\text{Ac}_2\text{O},0}$  at the beginning of the reaction.

$$\Delta H_r = \frac{-Q_r \cdot \rho}{c_{\text{Ac}_2\text{O},0}} \quad (5)$$

The values of the heat capacity and the density used are listed in the [supplementary information](#).

## Results and discussion

In Fig. 3, the temperature profiles of the experimental series E1-E3 are plotted against the reactor length. In the experimental series E3 and a total flow rate of 18 ml/min, the reaction is already completed, as the outlet temperature is close to the inlet temperature. Hence, the heat of reaction is almost identical to the dissipated heat. In contrary, all reactions in series E1 were not complete due to the lower acid concentration and the last temperature sensor revealed the highest value except with 18 ml/min. The dissipated and non-dissipated heat is therefore relevant for the heat of reaction. Experiment E2, 18 ml/min was carried out twice resulting in a deviation in heat of reaction of only 0.64%, demonstrating the reproducibility of the experiments and analysis (Fig. 3, middle left).

Furthermore, Fig. 3 shows the influence of the nitric acid concentration, which increases from 1.2 mol/l (E1) over 1.4 mol/l (E2) to 3.0 mol/l (E3). The differences in reaction rates are reflected in the temperature rise, which increases accordingly from E1 to E3. At low catalyst concentration and thus slow reaction rates, a temperature dip at the beginning of the reactor is clearly visible (Fig. 3, top and middle), which is presumably due to the enthalpy of mixing. At higher catalyst concentration and thus fast reaction rates as in E3 the dip cannot be seen in the profile (Fig. 3, bottom) as the enthalpy of mixing is overcompensated by the heat of reaction. The enthalpy of mixing can be determined when plotting the conversion against the enthalpy, as shown in Fig. 4. For this analysis, only the results of E1 and E2 are used, which have a conversion <100%, so that the measuring points are well distributed over the conversion range.

Since the heat of reaction is 0 kJ/kg at 0 conversion, the intercept is equal to the enthalpy of mixing and can be identified in Fig. 4. The enthalpy of reaction is calculated from eqs. 2–5. If the regression curve is shifted by the enthalpy of mixing, the enthalpy of reaction can be simply read at complete conversion. The value obtained for the heat of reaction correlates with the slope of the regression curve in Fig. 4.

For the model reaction applied in this study, Ładosz et al. [18] have determined a mixing enthalpy of  $8.8 \pm 2.1$  kJ/mol and a reaction enthalpy of  $-63 \pm 3.0$  kJ/mol in a continuous microreactor. These values agree with the measured values of  $7.2 \pm 2.8$  kJ/mol and  $-60.8 \pm 2.5$  kJ/mol. Since no catalyst was used in Ładosz et al. [18] and we used 1.2 or 1.4 mol/l HNO<sub>3</sub>, the catalyst plays only a minor role in the determination of the enthalpy of mixing. Interestingly, an exothermic enthalpy of mixing at 25 °C was determined in two studies for the same reaction but using batch reactors instead of a flow calorimeter [16, 17]. Furthermore, the enthalpy of mixing

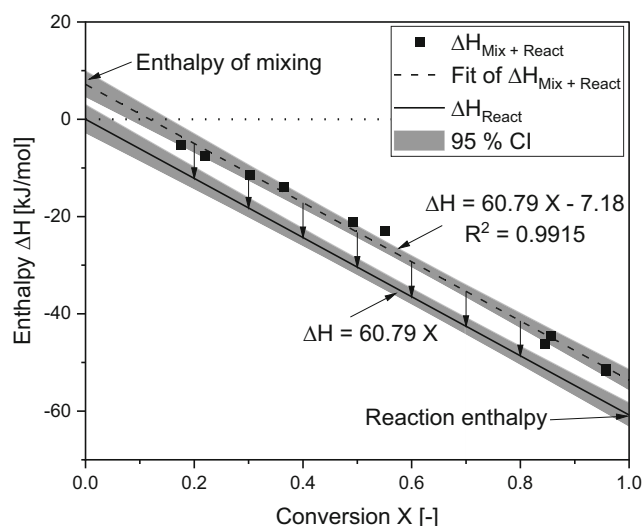


**Fig. 4** The measured enthalpies are plotted against the conversion. The intercept of the regression shows the enthalpy of mixing since there is no reaction. If the regression curve is shifted by the intercept as indicated, the enthalpy of reaction can be read at 100% conversion. The grey shaded areas show the 95% confidence interval (CI) of the regression curves

might depend on the mixing ratio of the substances [23]. We speculate that the range of reported values are explained by both the reactor type and various mole fractions. Batch experiments were conducted at a low mole fraction ( $\chi_{\text{Ac}_2\text{O}}/(\text{H}_2\text{O}+\text{Ac}_2\text{O}) = 0.006$ ) [16, 17], whereas continuous flow calorimeter results are recorded at  $\chi_{\text{Ac}_2\text{O}}/(\text{H}_2\text{O}+\text{Ac}_2\text{O}) = 0.02$  [18] and  $\chi_{\text{Ac}_2\text{O}}/(\text{H}_2\text{O}+\text{Ac}_2\text{O}) = 0.2$  (this work), respectively. We conclude that mixing enthalpy determinations at conditions close to production are important for a safe scale-up.

Compared to the setup used by Ładosz et al. [18], where the temperature was measured at the inlet zone and at two locations in the reaction zone in which isothermal conditions were assumed, the milli-calorimeter used in this study shows the temperature profile in the reactor. The temperature drop at the beginning of the profile at low acid concentrations confirms the endothermic enthalpy of mixing in continuous reactors. As the kinetics are included in the temperature profiles and since the heat transfer is precisely known for this reactor [12], the here presented results allow a clear prediction of the maximum temperature in an industrial plant scaled-up from the used milli-reactor.

The E3 experiment series resulted in a mean enthalpy of reaction of  $-54.5$  kJ/mol. Although we had expected a constant enthalpy of reaction, the individual determinations ranged from  $-61.5$  to  $-46.1$  kJ/mol. The origin of the observed deviation can be rationalised by the scheme shown in Fig. 5, where three arbitrary temperature profiles represent three cases with different flow rates. In case 1, the maximum peak is reached before the first temperature sensor (T1) and the reaction solution has cooled down at the first temperature probe already. Due to the mismatch of the position of the

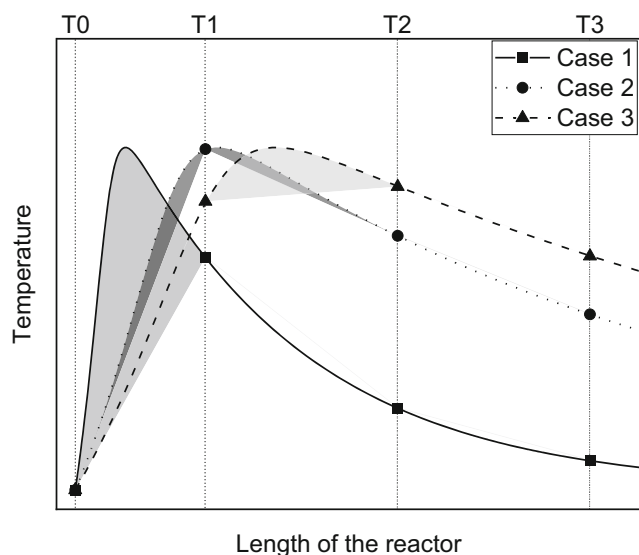


**Fig. 5** The figure shows three arbitrary temperature profiles. The shaded areas are lost in each case due to the interpolation. This area is the smallest when the temperature sensor is located at the maximum of the temperature profile

temperature probe and the position of the maximum temperature in the reactor, the shaded area between the temperature profile and the linear interpolation, which is used for the evaluation is lost for the calculation of the exchanged power. This area is the smallest for case 2, where the highest temperature is found at the same position as the first thermocouple. In case 3, where the maximum peak lies between sensor one and two, the reaction enthalpy is also underestimated.

To obtain an overlap of the maximum temperature and the thermocouple position, in E4 the total flow rates were increased stepwise by 4 ml/min between 36 and 72 ml/min.

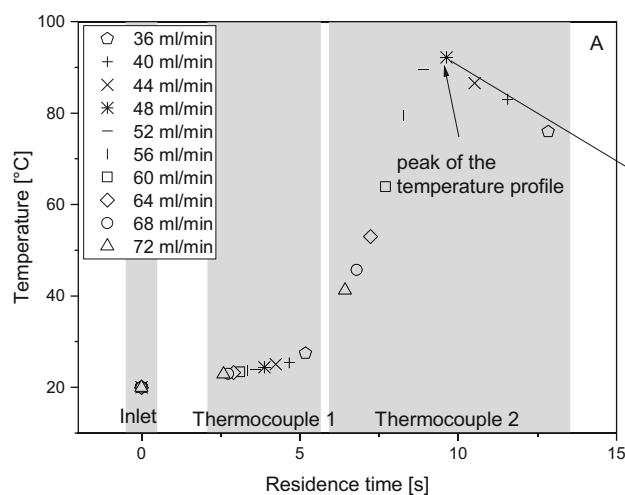


**Fig. 6** While the temperature measurements of E4 at the inlet are all taken at residence time 0, the residence times vary at different flow rates in the reactor. The shaded area indicates which thermocouple measured the temperature. The flow rate at which the highest temperature is

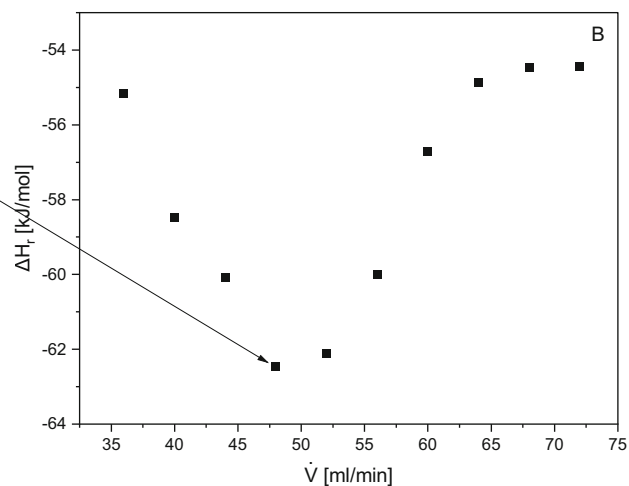
Obviously, the flow step size allows to adjust the uncertainty to the desired level. In Fig. 6A, the temperature of the first two thermocouples and the temperature of the inlet are plotted against the residence time. Apparently, at a higher flow rate, a particular thermocouple is reached faster, so that the residence time is shorter. It is demonstrated that the highest temperature is not detected at a high or low flow rate, so that the exothermicity of the reaction would be measured too low. At a flow rate of 48 ml/min, the second thermocouple detects exactly the highest temperature, which then leads to the most accurate calorimetric data.

According to the proposed model in Fig. 5, the reaction enthalpy calculated for the different flow rates shows a minimum at 48 ml/min (Fig. 6B). The observed enthalpy of reaction at 48 ml/min equals  $-62.5$  kJ/mol, which is in the literature range of  $-57$  [16] to  $-63$  kJ/mol [17].

Each flow rate was maintained for 4 minutes, so that the complete experiment with the 10 flow rates was completed after 40 minutes. With this method, the expensive installation of a fiber Bragg temperature sensor can be dispensed without compromising the quality of the result. Due to the fast and industry-oriented determination, the upscale can be carried out precisely, safely, and cost-effectively.

## Conclusion

When processes are scaled up, it is pivotal to know in advance how much energy a reaction will release. This data is preferably tested in a system that is already set up similarly to the production plant. In this way, predictions can be made more confidently. For example, the enthalpy of mixing was



measured at the position of thermocouple 2 is 48 ml/min (Diagram A). Diagram B shows that the highest exothermicity is also measured at 48 ml/min

determined as exothermic by two research groups in a batch reactor, while we measured the enthalpy of mixing as endothermic at 7.2 kJ/mol. This fact was explained by the different mole fractions of  $\text{Ac}_2\text{O}$  and different reactors used by the research groups. Since the batch reactors were operated as isothermally as possible, only small concentrations were used, whereas we can use significantly higher and industrially relevant concentrations with a polytropic reaction control.

Less nitric acid was used in the E1 and E2 series of experiments, so that the reaction proceeded relatively slow, and the linear interpolation depicted the effective temperature profile well. On the other hand, the determined reaction enthalpies of the fastest reaction with 3.0 mol/l  $\text{HNO}_3$  showed a standard deviation of 5.5 kJ/mol. This uncertainty results from the fact that the highest point of a temperature profile was not recorded with a temperature probe. Therefore, a facile and fast experiment scanning of different flow rates was performed, where the highest temperature was recorded. The enthalpy of reaction could then be determined to be  $-62.5$  kJ/mol, which is in the literature range of  $-57$  [16] to  $-63$  [17] kJ/mol. With the variation of the flow rate and the inline analysis, calorimetric data can be analysed accurately for reactions with a half-life of a few seconds to minutes.

In this work we presented a procedure to determine the heat of mixing and reaction accurately, simultaneously and continuously, such that predictions can be made more confidently.

**Symbols**  $A$ , heat transfer surface [ $\text{m}^2$ ];  $\beta$ , flow factor [ $\text{K ml min}^{-1}$ ];  $c_{\text{Ac}_2\text{O},0}$ , initial concentration of the limiting reactant  $\text{Ac}_2\text{O}$  [ $\text{mol m}^{-3}$ ];  $c_p$ , specific heat capacity [ $\text{J kg}^{-1} \text{K}^{-1}$ ];  $D_i$ , inner diameter [ $\text{m}$ ];  $\Delta H_r$ , reaction enthalpy [ $\text{J mol}^{-1}$ ];  $\Delta H_{\text{mix}}$ , mixing enthalpy [ $\text{J mol}^{-1}$ ];  $k$ , overall heat transfer coefficient [ $\text{W m}^{-2} \text{K}^{-1}$ ];  $L$ , length [ $\text{m}$ ];  $m$ , mass flow rate [ $\text{kg s}^{-1}$ ];  $n$ , number of segments [-];  $Q$ , heat [ $\text{J}$ ];  $Q_{\text{ex}}$ , exchanged heat flow [ $\text{W}$ ];  $Q_{\text{nex}}$ , non-exchanged heat flow [ $\text{W}$ ];  $Q_r$ , specific heat of reaction [ $\text{J kg}^{-1}$ ];  $Q_{\text{r}}$ , heat flow of reaction [ $\text{W}$ ];  $T$ , temperature [ $\text{K}$ ];  $t$ , time [ $\text{s}$ ];  $\Delta T$ , temperature difference [ $\text{K} / ^\circ\text{C}$ ];  $\Delta T_{\text{ad}}$ , adiabatic temperature increase [ $\text{K} / ^\circ\text{C}$ ];  $V$ , reactor volume [ $\text{m}^3$ ];  $\dot{V}$ , volume flow rate [ $\text{m}^3 \text{s}^{-1}$ ];  $X$ , conversion [-]

**Greek symbols**  $\rho$ , density of the reaction mixture [ $\text{kg m}^{-3}$ ];  $\chi$ , mole fraction [-]

**Abbreviations**  $\text{Ac}_2\text{O}$ , acetic anhydride;  $\text{AcOH}$ , acetic acid; AS, aqueous solution; CI, confidence interval; E1-E4, experimental series; FTIR, Fourier transform infrared spectrometer;  $\text{HNO}_3$ , nitric acid;  $\text{H}_2\text{O}$ , water; HTM, heat transfer medium; T0-T10, temperature measurements

**Supplementary Information** The online version contains supplementary material available at <https://doi.org/10.1007/s41981-022-00237-x>.

**Funding** Open access funding provided by ZHAW Zurich University of Applied Sciences. The work at the ZHAW is co-funded by Innosuisse, 38227.1 IP-ENG.

**Data availability** At ZHAW for the next 10 years.

**Code availability** At ZHAW.

## Declarations

**Conflicts of interest/Competing interests** The authors have no conflicts of interest to declare that are relevant to the content of this article. The authors Marlies Moser and Alain Georg work in the research department of the company that produces the flow calorimeter used in this study. In detail, Marlies Moser supported the literature search and the reaction planning. Alain Georg assisted with the evaluation and the analysis of the measured data.

**Consent to participate** Yes

**Consent for publication** Yes

**Open Access** This article is licensed under a Creative Commons Attribution 4.0 International License, which permits use, sharing, adaptation, distribution and reproduction in any medium or format, as long as you give appropriate credit to the original author(s) and the source, provide a link to the Creative Commons licence, and indicate if changes were made. The images or other third party material in this article are included in the article's Creative Commons licence, unless indicated otherwise in a credit line to the material. If material is not included in the article's Creative Commons licence and your intended use is not permitted by statutory regulation or exceeds the permitted use, you will need to obtain permission directly from the copyright holder. To view a copy of this licence, visit <http://creativecommons.org/licenses/by/4.0/>.

## References

- Pashkova A, Greiner L (2011) Towards small-scale continuous chemical production: technology gaps and challenges. *Chem Ing Tech* 83:1337–1342. <https://doi.org/10.1002/CITE.201100037>
- Doyle BJ, Elsner P, Gutmann B, Hannaerts O, Aellig C, Macchi A, Roberge DM (2020) Mini-monoplant technology for pharmaceutical manufacturing. *Org Process Res Dev* 24:2169–2182. <https://doi.org/10.1021/acs.oprd.0c00207>
- Hessel V, Vural Gürsel I, Wang Q, Noël T, Lang J (2012) Potential analysis of smart flow processing and micro process technology for fastening process development: use of chemistry and process design as intensification fields. *Chem Eng Technol* 35:1184–1204. <https://doi.org/10.1002/CEAT.201200038>
- Ebrahimi F, Kolehmainen E, Turunen I (2009) Safety advantages of on-site microprocesses. *Org Process Res Dev* 13:965–969. <https://doi.org/10.1021/OP900079F>
- Stoessel F (2009) Planning protection measures against runaway reactions using criticality classes. *Process Saf Environ Prot* 87:105–112. <https://doi.org/10.1016/J.PSEP.2008.08.003>
- Kummer A, Varga T (2019) Completion of thermal runaway criteria: two new criteria to define runaway limits. *Chem Eng Sci* 196:277–290. <https://doi.org/10.1016/J.CES.2018.11.008>
- Mortzfeld F, Polenik J, Guélat B, Venturoni F, Schenkel B, Filippini P (2020) Reaction calorimetry in continuous flow mode: a new approach for the thermal characterization of high energetic and fast reactions. *Org Process Res Dev* 24:2004–2016. <https://doi.org/10.1021/acs.oprd.0c00117>
- Schneider MA, Stoessel F (2005) Determination of the kinetic parameters of fast exothermal reactions using a novel microreactor-based calorimeter. *Chem Eng J* 115:73–83. <https://doi.org/10.1016/J.CEJ.2005.09.019>

9. Reichmann F, Millhoff S, Jirmann Y, Kockmann N (2017) Reaction calorimetry for exothermic reactions in plate-type microreactors using seebeck elements. *Chem Eng Technol* 40: 2144–2154. <https://doi.org/10.1002/CEAT.201700419>
10. Maier MC, Leitner M, Kappe CO, Gruber-Woelfler H (2020) A modular 3D printed isothermal heat flow calorimeter for reaction calorimetry in continuous flow. *React Chem Eng* 5:1410–1420. <https://doi.org/10.1039/D0RE00122H>
11. Zhang JS, Zhang CY, Liu GT, Luo GS (2016) Measuring enthalpy of fast exothermal reaction with infrared thermography in a microreactor. *Chem Eng J* 295:384–390. <https://doi.org/10.1016/J.CEJ.2016.01.100>
12. Moser M, Georg AG, Steinemann FL, Rütli DP, Meier DM (2021) Continuous milli-scale reaction calorimeter for direct scale-up of flow chemistry. *J Flow Chem* 11:691–699. <https://doi.org/10.1007/s41981-021-00204-y>
13. Frede TA, Maier MC, Kockmann N, Gruber-Woelfler H (2022) Advances in continuous flow calorimetry. *Org Process Res Dev* 26:267–277. <https://doi.org/10.1021/acs.oprd.1c00437>
14. Strotman NA, Tan Y, Powers KW, Soumeillant M, Leung SW (2018) Development of a safe and high-throughput continuous manufacturing approach to 4-(2-hydroxyethyl)thiomorpholine 1, 1-dioxide. *Org Process Res Dev* 22:721–727. <https://doi.org/10.1021/ACS.OPRD.8B00100>
15. Sans V, Cronin L (2016) Towards dial-a-molecule by integrating continuous flow, analytics and self-optimisation. *Chem Soc Rev* 45:2032–2043. <https://doi.org/10.1039/C5CS00793C>
16. Becker F, Walisch W (1965) Isotherme Kalorimetrie mit automatisch gesteuerter Peltier-Kühlung und fortlaufender Integration der Kompensationsleistung. *Z Phys Chem* 46:279–293. [https://doi.org/10.1524/zpch.1965.46.5\\_6.279](https://doi.org/10.1524/zpch.1965.46.5_6.279)
17. Zogg A, Fischer U, Hungerbühler K (2003) A new small-scale reaction calorimeter that combines the principles of power compensation and heat balance. *Ind Eng Chem Res* 42:767–776. <https://doi.org/10.1021/IE0201258>
18. Ładosz A, Kuhnle C, Jensen KF (2020) Characterization of reaction enthalpy and kinetics in a microscale flow platform. *React Chem Eng* 5:2115–2122. <https://doi.org/10.1039/D0RE00304B>
19. Conn JB, Kistiakowsky GB, Roberts RM, Smith EA (1942) Heats of organic reactions: XIII. Heats of hydrolysis of some acid anhydrides. *J Am Chem Soc* 64:1747–1752. <https://doi.org/10.1021/JA01260A001>
20. Dyne SR, Glasser D, King RP (1966) Automatically controlled adiabatic reactor for reaction rate studies. *Rev Sci Instrum* 38:209. <https://doi.org/10.1063/1.1771357>
21. Shatynski JJ, Hanesian D (1993) Adiabatic kinetic studies of the cytidine/acetic anhydride reaction by utilizing temperature versus time data. *Ind Eng Chem Res* 32:594–599. <https://doi.org/10.1021/IE00016A004>
22. Glasser D, Williams DF (1971) The study of liquid-phase kinetics using temperature as a measured variable. *Ind Eng Chem Fundam* 10:516–519. <https://doi.org/10.1021/I160039A027>
23. Haase R, Steinmetz P, Dücker KH (1972) Mischungsenthalpien beim flüssigen System Wasser + Essigsäure. *Zeitschrift für Naturforsch - Sect A J Phys Sci* 27:1527–1529. <https://doi.org/10.1515/zna-1972-1028>

**Publisher's note** Springer Nature remains neutral with regard to jurisdictional claims in published maps and institutional affiliations.